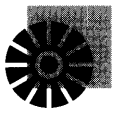

Contributed Paper

# Development of a Laser-Pumped X-Ray Laser with Full Spatial Coherence

NAGASHIMA Keisuke, TANAKA Momoko, NISHIKINO Masaharu, KISHIMOTO Maki, KADO Masataka, KAWACHI Tetsuya, HASEGAWA Noboru, OCHI Yoshihiro, SUKEGAWA Kota and TAI Renzhong

*Advanced Photon Research Center, Japan Atomic Energy Research Institute*
*8-1 Umemidai, Kizu-cho, Souraku-gun, Kyoto 619-0215, Japan*

(Received 13 November 2003 / Accepted 26 January 2004)

A laser-pumped x-ray laser with full spatial coherence has been developed for the first time. This x-ray laser has a wavelength of 13.9 nm and a beam divergence of 0.2 mrad. In the experiment, a seeding light from the first laser medium was amplified in the second medium, which worked as an active spatial filter. The observed beam divergence was close to the diffraction limited value within a factor of two. The seeding light was amplified in the second medium without refraction influence. The gain region of the second medium was far away from the target surface compared with that of the first medium, and was located in a region of considerably low density. From the measurement of visibility, it was found that the spatial coherent length was longer than the beam diameter. This means that this x-ray laser beam has full spatial coherence.

**Keywords:**
x-ray laser, spatial coherence, beam divergence, diffraction limit, refraction, visibility

## 1. Introduction

Lasing in a soft x-ray region was demonstrated for the first time in 1984 [1], Since then, x-ray lasers have been developed actively to improve the laser beam properties [2] and create compact devices [3,4]. Recently, a new scheme for an x-ray laser [5] was proposed by using an ultra-short pulse laser as a pumping source. In this scheme, which is called transient collisional excitation (TCE), target materials are irradiated by two laser pulses, a long prepulse for ionization and a short main pulse for excitation. The TCE scheme has facilitated much progress in collisional excitation x-ray lasers, and resulted in higher gain coefficients of a few tens per centimeter and shorter pulse durations less than 10 ps [6,7]. Saturated amplification, with a medium length less than 1 cm, was also achieved [8]. However, a medium with high gain was made in a high density region near the critical density for the pumping laser, where the density gradient was large. As a result, the x-ray laser was bent and diverged by refraction. Due to this refraction influence, the beam divergence of the x-ray lasers is over 1 mrad [9,10]. In order to suppress this influence, double massive targets [11,12] and a curved target [13] were applied, but the improvement was not satisfactory. In general, a beam with small divergence has high spatial coherence, which is the most important property for lasers. But, no beam with sufficient coherence has been generated up to now [14,15]. Recently, a compact laser at 46.9 nm with high spatial coherence was developed by use of discharge plasmas [16]. However, it appears difficult to shorten the wavelength by this method.

Here, we describe experimental results of a laser-pumped x-ray laser at 13.9 nm using the TCE scheme. In order to generate coherent x-ray light, we created two x-ray laser media by using two pumping laser beams and two targets. In this double target experiment, an x-ray laser from the first target was used as a seeding light and the coherent portion of the seeding light was amplified in the second medium. In this case, the amplifier (the second medium) works as an active spatial filter. If refraction is neglected, a condition for obtaining a single mode beam (where the spatial coherent length is longer than the beam diameter) is given by the relation $\lambda/d > d/L$ [17], where $\lambda$, $d$, and $L$ are the wavelength of the x-ray laser, the diameter of the media, and the distance between the two targets, respectively. We estimated that this condition for $\lambda$ = 13.9 nm was satisfied with the target distance of $L > 18$ cm using $d$ = 50 μm (this value was obtained from the previous experiment [18]). The most important point was how to reduce the refraction influence, which was caused by the density gradient in plasma. We succeeded in avoiding this influence by making a gain region in the lower density area. This is the first demonstration of

*author's e-mail: nagasima@apr.jaeri.go.jp*
*This article is based on the invited talk at the 20th Annual Meeting of JSPF (Nov. 2003, Mito).*

the laser-pumped x-ray laser with full spatial coherence [19].

## 2. Experimental Setup

In this experiment, the pumping laser was focused in a line shape and used to irradiate a silver target for generating an x-ray laser, the wavelength of which was 13.9 nm. We developed a pumping laser system, a hybrid system using Ti:sapphire and Nd:glass as laser media [20]. In this system, the Ti:sapphire oscillator generates femtosecond laser pulses at a wavelength of 1053 nm. The pulse is expanded temporally in the pulse stretcher, and it is amplified up to a few mJ in the Ti:sapphire regenerative amplifier. Then the pulse is divided into two: a prepulse for generating plasma and a main pulse for generating population inversion. These pulses are amplified in the Nd:glass amplifier and sent to the pulse compressor. Final pulse shape from the compressor consists of a long prepulse with a few hundreds ps and an intense short pulse with a few ps. The laser beam is spatially divided into two before the final-stage of the Nd:glass amplifier, and, finally, two beams of the pumping laser are generated.

The line focus was made by reflecting optics using a parabolic mirror and a spherical mirror [21]. The line width was about 20 μm and the length was 6.5 mm. Because the duration with high gain is less than 10 ps for the TCE [22], it is shorter than the duration when the x-ray light needs to pass through the laser medium (~20 ps). Thus, if the target is irradiated at the same time, the gain decreases before the light passes through the medium. In order to solve this problem, we used traveling wave pumping, in which the timing of generating the gain medium was matched to the propagation of x-ray laser light [22].

A schematic configuration of the double target experiment is shown in Fig.1. The distance between the two targets was 0.2 m. The pumping laser to the first target consisted of a prepulse with a 300 ps duration and a main pulse with a 4 ps duration. The total energy was 11 J and the energy ratio was 1:8. The pumping laser to the second target consisted of a prepulse with a 300 ps duration and a main pulse with a 12 ps duration. The total energy of the laser was 13.5 J and it had the same energy ratio. The main pulse was delayed 600 ps from the prepulse in both cases. We used the traveling wave pumping to the first target but not to the second target. The seeding light from the first target had a beam divergence of about 6 mrad. Consequently, the beam diameter was 1.2 mm at the second target position; this value was larger than the medium size, which was about 50 μm [18]. The pumping laser to the second target was delayed from that to the first target, and this delay time was changed by using an optical delay line. When the delay time, $\Delta t$, was 667 ps, it was equal to the value of the target distance divided by light speed.

## 3. Experimental Results

The x-ray laser beam profiles obtained in the double target experiments strongly depended on the delay time. Figure 2(a) shows a profile (a far field image) measured at $\Delta t$ = 667 ps at the position of 0.74 m from the second target. A bright region, which is the amplified light, is observed against the background of the seeding light. A shadow of the second target plasma is observed on the target surface, which is marked by a white line. This shadow was made by absorption of the seeding light by the second target plasma. Grid-shaped shadows are caused by the backing mesh of a zirconium filter, which is located at 0.2 m from the second target. In this case, both of the two media were generated in a high density region with an electron density over $10^{20}$ $cm^{-3}$ [22], where the density gradient was large. The observed beam profile spreads, particularly, in the horizontal direction, and the beam position is far away from the plasma shadow. This means that the beam is bent by refraction. The refraction angle is about 3 mrad. Based on measurement of a near-field image, the gain region was located at about 40 μm from the target surface [18].

When the delay time was shorter than 667-5 ps, another bright region was observed near the plasma shadow. Figure 2(b) shows a profile measured at $\Delta t$ = 667-15 ps at a position 2.81 m from the second target. We can observe a very bright and narrow beam profile, the divergence of which is 0.2 mrad (FWHM). This divergence is one thirtieth of that from the

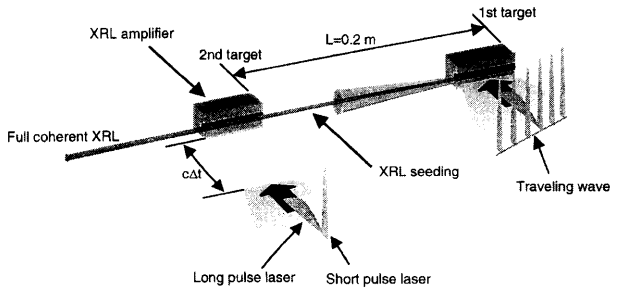


Fig. 1 Schematic configuration of the double target experiment. The distance between the two targets, L is 20 cm and the timing between the two pumping lasers is delayed with $\Delta t$. The pumping laser is the traveling wave for the first target but not for the second target.

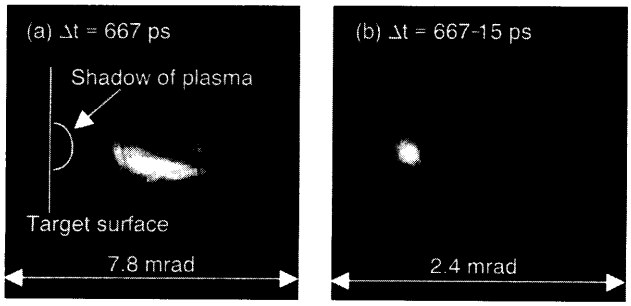


Fig. 2 X-ray laser beam profiles measured by the x-ray CCD camera in the double target experiments. The profiles were measured at 0.74 m (a) and 2.81 m (b) from the second target position. The target length was 6.5 mm.

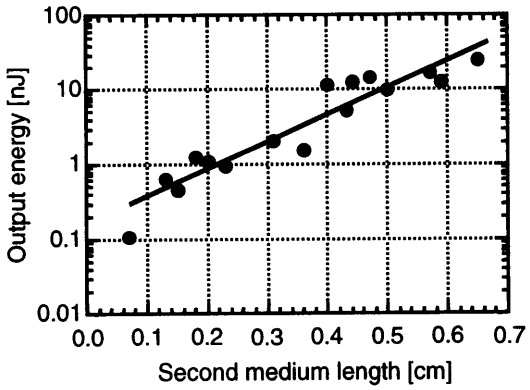


Fig. 3 Output energy of the narrow x-ray laser beam plotted with the second medium length.

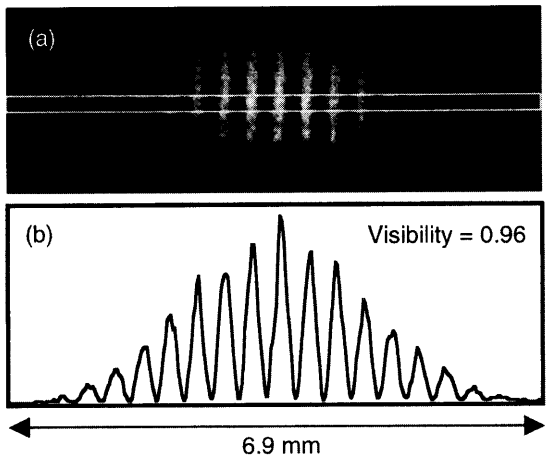


Fig. 4 Interference pattern with the slit distance of 150 μm. Law data obtained from the x-ray CCD camera (a) and a line plot of the fringe (b). The second target length was 6.5 mm.

single target, and is the smallest value of x-ray lasers. The x-ray laser beam is isotropic and has a nearly Gaussian profile. The important point is the location of this beam, which is about 100 μm from the target surface and just on the shadow of the second target plasma. This means that this narrow x-ray laser beam is *not* bent by refraction. Thus, the refraction angle is smaller than the beam divergence.

The output energy of the narrow x-ray laser beam is plotted with the second medium length in Fig.3. The energy increases exponentially with the medium length. The gain coefficient is estimated to be 7.9 $cm^{-1}$. The gain-length product is 5.1 and the amplification factor is 170. These values are small compared with those obtained from the single target experiment [22]. In this experiment, the energy of the seeding light was 270 nJ and the coupling efficiency to the second medium was about 0.1 %, which was evaluated from the beam divergence as $(0.2/6)^2$. The output energy from the amplifier was 25 nJ and its intensity was lower than the saturation intensity by about two orders. This low intensity results from insufficiencies of the second target length and the seeding light intensity. If we create a second medium with a length of 1 cm (it should be pumped by the traveling wave) and an injection of seeding light with saturation intensity, we can expect an amplified beam with saturation intensity.

The beam with small divergence has high spatial coherence. Here we carried out a Young's double slit experiment in order to measure the spatial coherence of the narrow x-ray laser beam. The double slits, with a width of 16 μm and a separation distance of 150–350 μm, were located at 2.3 m from the second target. The beam size was 460 μm at the slits' position. We observed the x-ray interference pattern at 3.9 m from the slits' position using an x-ray CCD camera. Figure 4 shows an interference pattern with a slit distance of 150 μm. The visibility of the interference is defined as $V = (I_{max}-I_{min})/(I_{max}+I_{min})$, where $I_{max}$ and $I_{min}$ are maximum and minimum values of the interference pattern, respectively. The visibility of the fringe shown in Fig.4 is 0.96. Figure 5 shows the dependence of visibility on the slit distance. The visibilities are not different between the

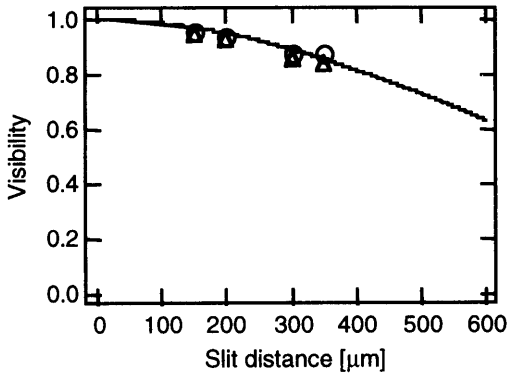


Fig. 5 Visibility plotted with the slit distance. The symbols of circle and triangle represent values in the directions perpendicular and parallel to the target surface, respectively. The line shows a Gaussian fitting to the data points.

directions perpendicular (the circles) and parallel (the triangles) to the target surface, which means the x-ray beam is isotropic from the view point of spatial coherence. From the figure, the visibility is about 0.8 at a slit distance of 460 μm, which is the beam size. Considering a monochromatic light source with a Gaussian intensity profile, the relation between the visibility and the spatial coherent length, $L_C$, is given by $V(\Delta x) = \exp(-\Delta x^2/2L_C^2)$, where $\Delta x$ is the slit distance [23]. From the fitting shown in Fig.5, the spatial coherent length is estimated to be about 600 μm, and it is larger than the beam size. Therefore, this x-ray laser beam satisfies the condition for full spatial coherence.

## 4. Analysis

The spatial quality of a laser beam is measured by comparing it with the diffraction limit. The narrow x-ray beam obtained here has an intensity profile of a nearly Gaussian shape. The diffraction limited divergence (FWHM) of the

Gaussian beam is given by

$$\theta_{\mathrm{FWHM}} = \frac{2\ln 2}{\pi}\frac{\lambda}{d_0}, \tag{1}$$

where $d_0$ is the FWHM of the laser intensity at the beam waist. From the previous result, $d_0$ = 50 μm [19], we estimated $\theta_{\mathrm{FWHM}}$ = 0.12 mrad and found that the measured divergence of 0.2 mrad is in a range smaller than two times the theoretical limit.

In the double target experiment, the second medium works as a spatial filter. Here we calculate the effect of diffraction by this spatial filter using a diffraction integral of

$$U(P) = \frac{i}{\lambda}\iint g_0(x_0, y_0)\frac{\exp(-iks_0)}{s_0} g(x, y)\frac{\exp(-iks)}{s}\,\mathrm{d}x_0\mathrm{d}y_0\mathrm{d}x\mathrm{d}y, \tag{2}$$

where the light source with a profile of $g_0(x_0, y_0)$ is placed at the first target position and the spatial filter with a transmission profile of $g(x, y)$ is placed at the second target position. The symbols of s and $s_0$ represent the distances from the point $(x_0, y_0)$ to the point $(x, y)$, and from the point $(x, y)$ to the point $P$. The beam divergence is calculated from the field amplitude, $U(P)$, at the position of $P$, which is far from the second target. Figure 6 shows a calculated result assuming that $g_0$ is a point source and $g(x, y)$ is a Gaussian shape with the given diameter (the solid line). In this case, the minimum value is 0.25 mrad, which is larger than the measured value. When we consider a finite source size, this line becomes close to the measured point. Thus, the measured divergence is proper in this theoretical viewing point.

The deterioration of the beam divergence and the spatial coherence is mainly an effect of refraction resulting from the density gradient in plasma. Here we consider that the x-ray light propagates in a parallel direction from the target surface, and the density gradient exists only in the perpendicular direction. In this case, the refractive index, $n$, is a function depending on the perpendicular position. The refraction angle is

$$\theta = \frac{\mathrm{d}x}{\mathrm{d}z} = \frac{\nabla n}{n} L, \tag{3}$$

where $x$ and $z$ are the positions perpendicular and parallel to the target surface, respectively, and $L$ is the propagation length in the $z$ direction. The refractive index in plasma is given by

$$n = \sqrt{1 - \alpha\frac{n_e}{n_{cr}}}, \tag{4}$$

where $n_e$ and $n_{cr}$ are the plasma electron density and the critical density for the pumping laser, respectively, and $\alpha$ = $(13.9/1053)^2$. Assuming an exponential density profile of $n_e$ = $n_{cr}\exp(-x/L_n)$, the refraction angle is

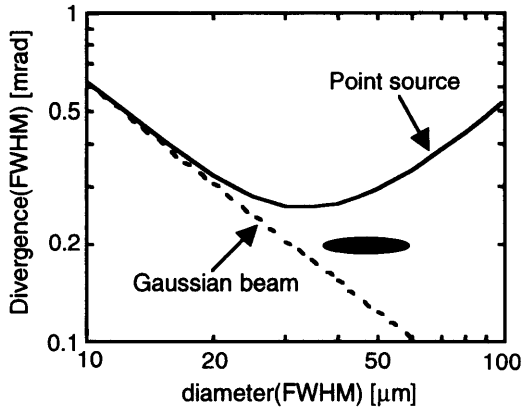


Fig. 6 Diffraction limited divergence of the Gaussian beam (the dot line) and the divergence calculated from the diffraction integral assuming a point source (the solid line). The solid symbol is the experimental point of 0.2 mrad.

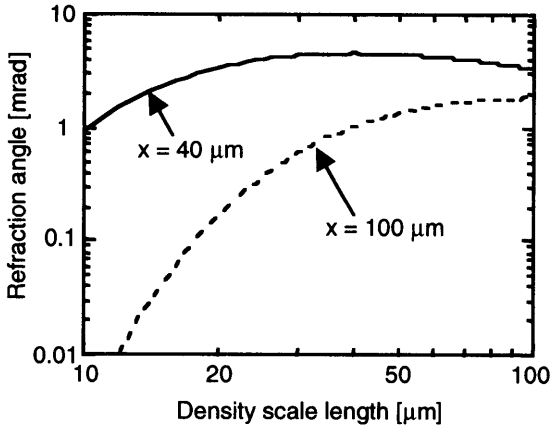


Fig. 7 Calculated refraction angle as a function of the density scale length. The two lines (the solid and the dot) are cases for the spread beam (Fig.2(a)) and the narrow beam (Fig.2(b)).

$$\theta = \frac{\alpha L}{2L_n}\exp\left(-\frac{x}{L_n}\right), \tag{5}$$

where $L_n$ is the scale length determining the density profile. Figure 7 shows calculated refraction angles from the above equation. In the case shown in Fig.2(a) (the spread beam), the perpendicular position at the medium was 40 μm from the target surface [18] and the measured refraction angle was 3 mrad. In the case shown in Fig.2(b) (the narrow beam), the perpendicular position at the medium was about 100 μm and the refraction angle was less than 0.2 mrad. From a comparison of calculated and measured values, the density scale length was estimated to be about 20 μm. The results of this analysis indicate that the electron density at the second medium (for the narrow beam) is about 1 % of the critical density. This is a considerably low value compared with previously reported results [22].

## 5. Conclusions

We demonstrated, for the first time, a laser-pumped x-ray laser with full spatial coherence at 13.9 nm. A very narrow x-ray laser beam with a divergence of 0.2 mrad was generated in a double target experiment, in which a seeding light from the first medium was amplified in the second medium. This beam divergence is the smallest value of x-ray lasers and is close to the diffraction limited value, within a factor of two. The essential point of this result is that the seeding light is amplified in the second medium without refraction influence. It is possible to generate an x-ray laser with full spatial coherence and saturation intensity by making a longer second medium with a length of about 1 cm using traveling wave pumping.

## Acknowledgements

The authors would like to acknowledge the support and encouragement of T. Kimura, T. Tajima, and Y. Kato. We are also grateful for fruitful discussions with H. Daido and K. Namikawa, and especially for the technical support of Y. Suzuki.

## References

[1] D.L. Matthews *et al.*, Phys. Rev. Lett. **54**, 110 (1985).
[2] A. Carillon *et al.*, Phys. Rev. Lett. **68**, 2917 (1992).
[3] S. Basu *et al.*, Appl. Phys. B **57**, 303 (1993).
[4] B.E. Lemoff *et al.*, Phys. Rev. Lett. **74**, 1574 (1995).
[5] V.N. Shlyaptsev *et al.*, SPIE **2012**, 212 (1993).
[6] P.V. Nickles *et al.*, Phys. Rev. Lett. **78**, 2748 (1997).
[7] J. Dunn *et al.*, Phys. Rev. Lett. **80**, 2825 (1998).
[8] M.P. Kalachnikov *et al.*, Phys. Rev. A **57**, 4778 (1998).
[9] H. Daido *et al.*, Opt. Lett. **20**, 61 (1995).
[10] J. Zhang *et al.*, Phys. Rev. Lett. **78**, 3856 (1997).
[11] C.L.S. Lewis *et al.*, Opt. Commun. **91**, 71 (1992).
[12] S. Wang *et al.*, J. Opt. Soc. Am. B **9**, 360 (1992).
[13] R. Kodama *et al.*, Phys. Rev. Lett. **73**, 3215 (1994).
[14] J.E. Trebes *et al.*, Phys. Rev. Lett. **68**, 588 (1992).
[15] R.E. Burge *et al.*, J. Opt. Soc. Am. B **15**, 2515 (1998).
[16] Y. Liu *et al.*, Phys. Rev. A **63**, 033802 (2001).
[17] R.C. Elton, *X-RAY LASERS* (Academic Press, 1990).
[18] M. Tanaka *et al.*, Surface Rev. Lett. **9**, 641 (2002).
[19] M. Tanaka *et al.*, Opt. Lett. **28**, 1681 (2003).
[20] T. Kawachi *et al.*, Appl. Opt. **42**, 2198 (2003).
[21] I.N. Ross *et al.*, Appl. Opt. **26**, 1584 (1987).
[22] T. Kawachi *et al.*, Phys. Rev. A **66**, 033815 (2002).
[23] L. Mandel and E. Wolf, *Optical coherence and quantum optics* (Cambridge University Press, New York, 1995).